The International Young Researchers' Conference
DOI: doi.org/10.34614/iyrc0052

Development of an aptamer-gold nanoparticle assay for field use in informing "DIY-HRT"

Arthur Liang, Sonya Ahuja, and Gwyn Uttmark
Stuyvesant High School, United States
aliang21@stuy.edu

Abstract

Most individuals on Feminizing Hormone Therapy receive their medications from a conventional supply chain. However, some utilize non-medical sources because they do not have access to medical care, have difficulty covering the cost, or distrust the medical establishment. Using a non-licensed supplier heightens the uncertainty that the hormone procured is the hormone received. Here, we aim to develop highly affinitive and selective aptamers for progesterone and testosterone for field-ready hormone detection "drug tests". A good aptamer is characterized by high sensitivity and specificity for a specific target so discrimination against interfering agents is important for minimizing false positives. Researchers have identified several promising features and motifs of nucleotide sequences, stems, loops, and three-way junctions that may amplify aptamer specificity for targets. As a part of our testing procedure, we analyzed several existing progesterone and testosterone aptamers and developed our own using the MFold Web Server. We then characterized their performance in a visible to the eye colorimetric gold-nanoparticle (AuNP) assay to identify several promising testosterone and progesterone aptamers for further testing.

Keywords: Gold Nanoparticles, Aptamers, DIY-HRT, Colorimetric Assay

Introduction

Some trans, gender non-conforming or gender queer people (here referred to broadly as trans) who are undergoing Feminizing Hormone Treatment (FHT) are unable or unwilling to purchase necessary hormones from official pharmacies because they do not have access to medical care, have financial problems, or distrust the medical establishment. In this paper, we focus on "DIY-HRT" within the trans population. A 2013 survey on Ontario transgender communities found that of the 433 surveyed, a quarter of those using hormones obtained them from non-medical sources such as the Internet, friends, and relatives [1]. However, there are often no feasible methods for verification that the intended hormone bought online is the hormone received. We aim to develop a cheap, field-ready, and rapid test for various hormones used by trans people outside of conventional medical institutions to aid them in making informed decisions. A colorimetric aptamer-based method for hormone detection is preferred for its high affinity, stability, and low production cost. Other mediums of detection such as liquid/gas chromatography-mass spectrometry or electrochemical methods have superior sensitivity rates but are expensive and complex [2].

The ideal assay enables detection of testosterone or progesterone in application relevant solutions without additional equipment.

In our design, an end-user can test their substance upon receipt with our aptamer-based assay. If the corresponding hormone is present in sufficient quantities, then the aptamers will dissociate from the AuNP surfaces and bind to the hormone, leaving the AuNPs to aggregate. The user will be able to visually detect a color change (or lack thereof) in the solution thus determining whether the solution contains the hormone they ordered.

Background

Single-stranded DNA aptamers (ssDNA aptamers) are oligonucleotides that bind a target ligand with millimolar to nanomolar efficiency and often, they have high specificity for a specific target. There are various methods to identify aptamers for specific targets. The most popular include SELEX (Systematic Evolution of Ligands by Exponential Enrichment) methods [3] which can be augmented with differing selection mediums (molecular beads, gold nanoparticles) [4]. Researchers have identified several promising features and motifs of nucleotide sequences, stems, loops, and three-way junctions that may amplify aptamer specificity for targets [5]. However, specific binding mechanisms often remain unknown because developing crystal or NMR structures is difficult and tedious. We currently cannot feasibly design an aptamer for a given target. SELEX selects the best aptamers in a pool of randomly generated aptamers. Often the selection schema doesn't select for differing lengths resulting in extraneous flanking nucleotides which can reduce binding affinity and/or assay performance [4].

A good aptamer is characterized by high sensitivity and specificity for a specific target. Discrimination against interfering agents is important for minimizing false positives.

Many high affinity and highly selective aptamers have been identified for some bioactive targets such as 17α-estradiol (E2, Figure 1) and glutamine [4]. Estradiol is of particular interest to us because it is used in Feminizing Hormone Therapies. Several anti-E2 aptamers have been developed for use in a AuNP assay, which uses aptamer-coated gold nanoparticles as a method to colorimetrically detect E2 in application relevant solutions (e.g. urine samples) [4]. When aptamer-coated AuNPs are introduced into a target solution, target-specific aptamers will preferentially bind the targets and dissociate from AuNP surfaces, leading to AuNP aggregation and a resulting color change. However, it has been found that complete dissociation is heavily dependent on whether or not the aptamer, along its entire length, preferentially binds the target [4]. The longer the aptamer, the more likely there will be flanking nucleotides from the non-binding complex of the aptamer that remain associated with the AuNPs, preventing aggregation and skewing measures of dissociation. Previous literature has demonstrated that splitting aptamers may improve AuNP based colorimetric sensitivity by increasing the detection limit [6, 7].

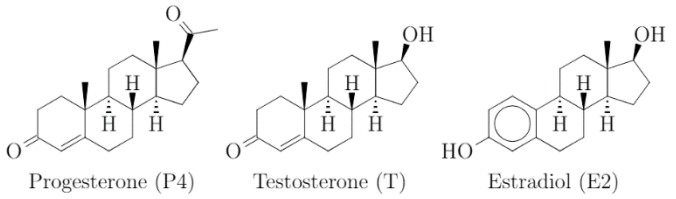

FIGURE 1. Progesterone, Testosterone and Estradiol are structurally similar hydrophobic steroids, aptamers specific to one of them will likely exhibit affinity for the other hormones as well.

In this paper, we focus on testosterone and progesterone (Figure 1). Both play key roles in the development of primary sexual characteristics as well as promoting secondary sexual characteristics. Generally speaking, testosterone is the primary masculinizing sexual hormone and promotes the growth of facial hair and muscle development. Per contra, progesterone plays a crucial role in feminine development by supporting breast development and suppressing endogenous testosterone production [8].

For transgender men and trans masculine individuals, testosterone often suppresses the

menstrual cycle and decreases estrogen production. Trans feminine individuals take progesterone supplements in order to promote the development of female secondary sex characteristics such as growth of the breasts, widening of the hips, and development of body hair especially in the pubic area.

Experimental

Aptamer Discovery

From past literature, we identified multiple existing aptamers that demonstrated affinity and selectivity for testosterone and progesterone. Of twelve aptamers we considered (Table 1) we chose two progesterone and one testosterone aptamers to investigate further.

Temperature sensitivity is not ideal because the aptamer assay should be tolerable to a broad range of conditions. Through several simulations, we eliminated Skouridou2017-T5 from our consideration (Figure S3). We also eliminated the Alhadrami2017-PG13 aptamer since the aptamer's 61 nucleotide sequence was previously truncated in its non-binding region for higher affinity [2].

JausetRubio2019-T6, in addition to having a low Kd value, exhibits high sensitivity for testosterone with a relatively low LOD value when compared to that of progesterone and estradiol (Table 1).

Kd is the equilibrium dissociation constant and it measures binding affinity, the strength of the interaction between a ligand and its target molecule. Binding affinity is influenced chiefly by intermolecular interactions such as hydrogen bonding and Van der Waals forces between the two molecules but is also affected by the presence of other molecules. The smaller the Kd value, the greater the binding affinity the ligand has for its target. LOD stands for limit of detection and is the lowest quantity of the target that can be distinguished from the absence of the target by the ligand. An effective aptamer assay requires a relatively small LOD value for the target molecule compared to the aptamer's LOD value for other biologically relevant molecules.

Aptamer Manipulation

Truncating and modifying existing aptamers has been previously shown to make them more selective and affinitive toward testosterone and progesterone [2, 4].

Past literature also suggests steric accessibility and structures such as stems, loops, and three-way junctions are important in allowing the aptamers to bind to small hydrophobic molecules like progesterone and testosterone [5]. We modified JausetRubio2019-T6 by trimming around the conspicuous hairpin in order to minimize the number of flanking nucleotides that may inhibit dissociation from AuNPs. JausetRubio2019-T6-57 includes, in addition to the main hairpin, one flanking base on each end and also the second, shorter hairpin. The second testosterone aptamer we designed, JausetRubio2019-T6-60, is similar but the second hairpin is novel and absent from the secondary structure of JausetRubio2019-T6 in the same conditions. Having more than one hairpin may amplify the aptamer's affinity for testosterone. The third testosterone aptamer we designed, JausetRubio2019-T6-46, is the shortest and includes the main hairpin and three flanking bases on each end. Finally, we noticed that the end sequence of the main hairpin strongly resembled the first structural motif described elsewhere [5] so we made three base substitutions when designing our fourth testosterone aptamer (JausetRubio2019-T6-54m, Figure 2) to include the motif.

We simulated how our modified aptamers would fold in specific temperature and salt conditions to identify any outstanding structural anomalies like the Skouridou2017-T5 aptamer (Figure S3). Notably, the main hairpin from the original aptamer was preserved in all four modified testosterone aptamers (Figure S2)

For the progesterone aptamers, PG13T1 and PG13T2 were aptamers truncated from PG13 in a previous paper [2].

TABLE 1. Aptamers reviewed from previous literature, bolded aptamers were tested.

Target	Aptamer	Target K_d (nM)	LOD (nM)		
			T	P4	E2
Testosterone	**JausetRubio2019-T6**	0.80 ± 0.18	103	1090	4725
	Skouridou2017-T5	4.0 ± 5.8	NR	NR	NR
	Skouridou2017-T4	1.2 ± 0.2	NR	NR	NR
	Skouridou2017-T3	1.8 ± 0.6	NR	NR	NR
	Skouridou2017-T2	33.2 ± 76.2	NR	NR	NR
Progesterone	**Alhadrami 2017-PG13T1**	2.1	NR	NR	NR
	Alhadrami 2017-PG13T2	2.2	NR	NR	NR
	Alhadrami 2017- PG13	35	NR	NR	NR
	Alhadrami 2017- PG13C4	NR	NR	NR	NR
	JausetRubio2019-P5	2.03 ± 3.24	1060	112	1373
	JausetRubio2019-P6	0.57 ± 0.84	1096	183	432

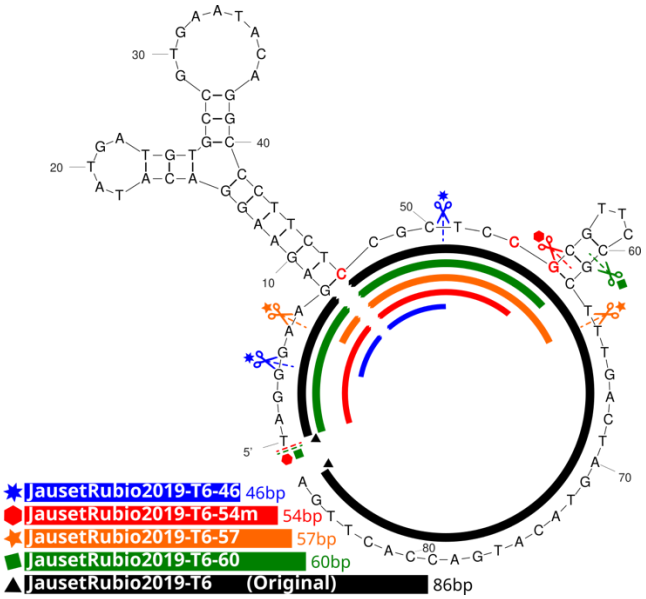

FIGURE 2. New testosterone aptamers derived from JausetRubio2019-T6.

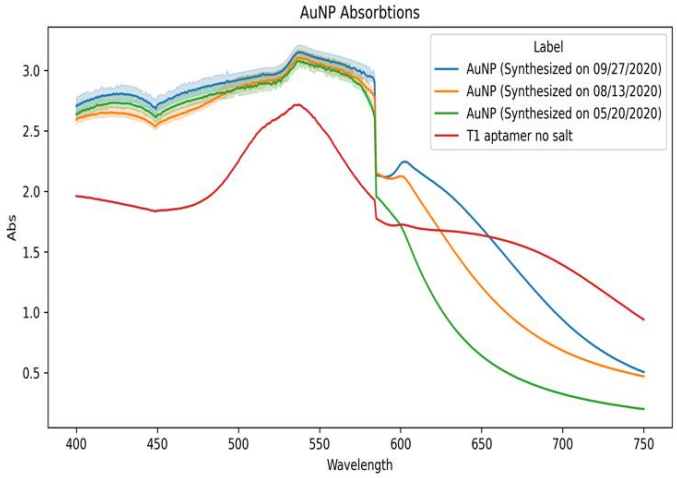

FIGURE 3. Bare AuNP Absorption Solution Spectra to Confirm Aptamer Affinity and Consistent AuNP Batching.

Methodology

Simulations

All secondary structure simulations were completed at 55mM Na+ and 25 degrees Celsius via the MFold web server [9].

Synthesis of AuNPs

AuNPs were synthesized via reduction of HAuCl4 with sodium citrate. An aqueous solution of HAuCl4 was stirred vigorously at reflux, and a solution of sodium citrate was added immediately in one batch. After boiling for 10 min, the solution was stirred for another 15 min at room temperature. The solution spectra were taken (Figure 3) to verify a successful and consistent synthesis and then stored at room temperature on a shaker for later use [4].

Titration

The solution was then centrifuged at 6000rpm for 10m and the supernatant was removed. The AuNPs were then re-suspended in an 23.8mM NaCl aqueous solution (Figure 4). 60nmol of the appropriate aptamer was added to the solutions for a 3:1 aptamer:particle ratio. The solutions were vortexed for 5 minutes. An aqueous 9pM P4 solution and 90pM E2 50:50 water:ethanol solution were used for the titrations. Titrations were performed at RT with a temperature control (Figure 5).

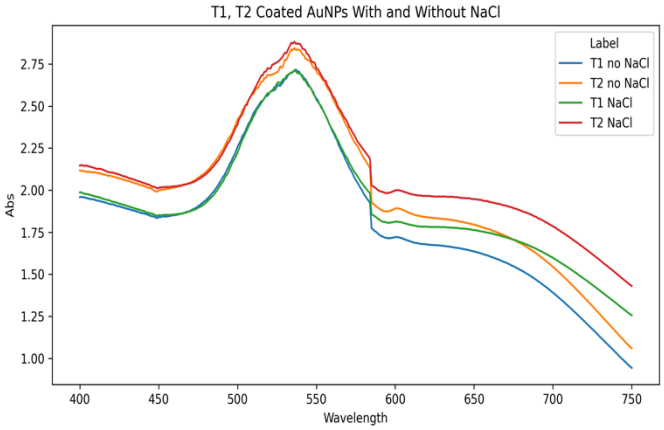

FIGURE 4. Coated AuNP Absorption Solution Spectra With and Without NaCl to Confirm AuNP Stabilization Against Salt-Mediated Aggregation.

Materials

We ordered all oligonucleotides from IDT (Integrated DNA Technologies). Progesterone and Estradiol were analytical grade powders from Sigma.

Results

All data were collected via a spectrophotometer and raw data was stored in a spreadsheet. The following graphs were produced using these spreadsheets in Python. All appeared normal as expected and no strong conclusions can be made without further analysis.

The three batches of AuNPs synthesized months apart have no clear disparities in their absorption spectra (Figure 3). This allows us to be more certain that the results from our experiment aren't due to inherent differences between different batches of AuNPs. Also, when we ran a batch of T1 aptamer-coated AuNPs through the spectrophotometer, we saw significant changes to the absorption spectra. This indicates that when aptamers are added, they bind to the gold nanoparticles and hinder aggregation. Here, we confirm that our aptamers exhibit affinity for the AuNPs in the first place.

Additionally, we obtained similar spectra shifts compared to previous literature when we added NaCl to the aptamer-coated AuNP solutions (Figure 4) [10, 11].

For all the titrations, increasing the concentrations of each hormone dilutes the solution, which we adjust for in the data analysis (Figure 5). When visually inspecting the absorption spectra, no trend immediately presents itself. Unfortunately due to COVID-19, we do not yet have results for our testosterone aptamers.

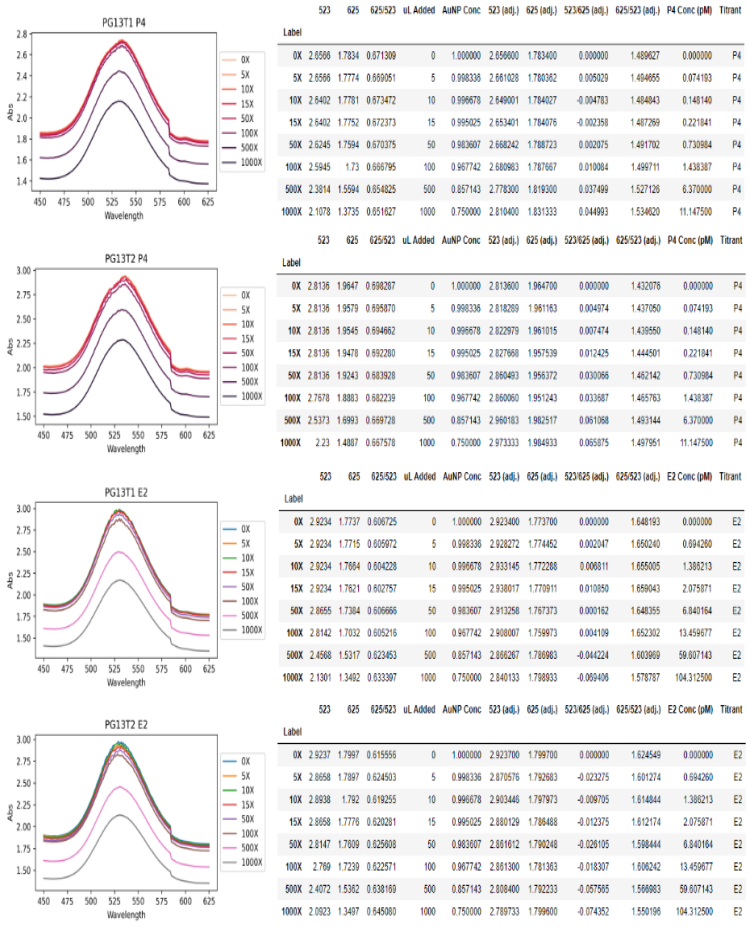

Label	523	625	625/523	uL Added	AuNP Conc	523 (adj.)	625 (adj.)	523/625 (adj.)	625/523 (adj.)	P4 Conc (pM)	Titrant
0X	2.6566	1.7834	0.671309	0	1.000000	2.656600	1.783400	0.000000	1.489627	0.000000	P4
5X	2.6566	1.7774	0.669051	5	0.998336	2.661028	1.780362	0.005029	1.494655	0.074193	P4
10X	2.6402	1.7781	0.673472	10	0.996678	2.649001	1.784027	-0.004783	1.484843	0.148140	P4
15X	2.6402	1.7752	0.672373	15	0.995025	2.653401	1.784076	-0.002358	1.487269	0.221841	P4
50X	2.6245	1.7594	0.670375	50	0.983607	2.668242	1.786723	0.002075	1.491702	0.730984	P4
100X	2.5945	1.73	0.666795	100	0.967742	2.680963	1.787667	0.010084	1.499711	1.438387	P4
500X	2.3814	1.5594	0.654825	500	0.857143	2.778300	1.819300	0.037499	1.527126	6.370000	P4
1000X	2.1078	1.3735	0.651627	1000	0.750000	2.810400	1.831333	0.044993	1.534620	11.147500	P4

Label	523	625	625/523	uL Added	AuNP Conc	523 (adj.)	625 (adj.)	523/625 (adj.)	625/523 (adj.)	P4 Conc (pM)	Titrant
0X	2.8136	1.9647	0.698287	0	1.000000	2.813600	1.964700	0.000000	1.432076	0.000000	P4
5X	2.8136	1.9579	0.695870	5	0.998336	2.818269	1.961163	0.004974	1.437050	0.074193	P4
10X	2.8136	1.9545	0.694662	10	0.996678	2.822979	1.961015	0.007474	1.439550	0.148140	P4
15X	2.8136	1.9478	0.692280	15	0.995025	2.827668	1.957539	0.012425	1.444501	0.221841	P4
50X	2.8136	1.9243	0.683928	50	0.983607	2.860493	1.956372	0.030066	1.462142	0.730984	P4
100X	2.7678	1.8883	0.682239	100	0.967742	2.860060	1.951243	0.033687	1.465763	1.438387	P4
500X	2.5373	1.6993	0.669728	500	0.857143	2.960183	1.982517	0.061068	1.493144	6.370000	P4
1000X	2.23	1.4887	0.667578	1000	0.750000	2.973333	1.984933	0.065875	1.497951	11.147500	P4

Label	523	625	625/523	uL Added	AuNP Conc	523 (adj.)	625 (adj.)	523/625 (adj.)	625/523 (adj.)	E2 Conc (pM)	Titrant
0X	2.9234	1.7737	0.606725	0	1.000000	2.923400	1.773700	0.000000	1.648193	0.000000	E2
5X	2.9234	1.7715	0.605972	5	0.998336	2.928272	1.774462	0.002047	1.650240	0.694260	E2
10X	2.9234	1.7664	0.604228	10	0.996678	2.933145	1.772288	0.006811	1.655005	1.389213	E2
15X	2.9234	1.7621	0.602757	15	0.995025	2.938017	1.770911	0.010850	1.659043	2.075871	E2
50X	2.8655	1.7384	0.606666	50	0.983607	2.913258	1.767373	0.000162	1.648355	6.840164	E2
100X	2.8142	1.7032	0.605216	100	0.967742	2.908007	1.759973	0.004109	1.652302	13.459677	E2
500X	2.4568	1.5317	0.623453	500	0.857143	2.866267	1.786983	-0.044224	1.603999	59.807143	E2
1000X	2.1301	1.3492	0.633397	1000	0.750000	2.840133	1.798933	-0.069406	1.578787	104.312500	E2

Label	523	625	625/523	uL Added	AuNP Conc	523 (adj.)	625 (adj.)	523/625 (adj.)	625/523 (adj.)	E2 Conc (pM)	Titrant
0X	2.9237	1.7997	0.615556	0	1.000000	2.923700	1.799700	0.000000	1.624549	0.000000	E2
5X	2.8658	1.7897	0.624503	5	0.998336	2.870576	1.792683	-0.023275	1.601274	0.694260	E2
10X	2.8938	1.792	0.619255	10	0.996678	2.903446	1.797973	-0.009705	1.614844	1.389213	E2
15X	2.8658	1.7776	0.620281	15	0.995025	2.880129	1.786488	-0.012375	1.612174	2.075871	E2
50X	2.8147	1.7609	0.625608	50	0.983607	2.861612	1.790248	-0.026105	1.598444	6.840164	E2
100X	2.769	1.7239	0.622571	100	0.967742	2.861300	1.781363	-0.018307	1.606242	13.459677	E2
500X	2.4072	1.5362	0.638169	500	0.857143	2.808400	1.792233	-0.057565	1.566983	59.807143	E2
1000X	2.0923	1.3497	0.645080	1000	0.750000	2.789733	1.799600	-0.074352	1.550196	104.312500	E2

FIGURE 5. Absorption Spectra and Data Points for Titrations of P4/E2.

We use the following to determine the Limit of Detection and to define an adjusted metric for colorimetric change.

$$\mathrm{LOD} = 3.3 \cdot S_{C_{\mathrm{Ligand}}} \cdot \sqrt{1 - (1 - R^2)\frac{n-1}{n-2}}$$

and

$$A_{\lambda_1:\lambda_{2_{\mathrm{adj}}}} = \frac{A_{\lambda_{1_{\mathrm{adj}}}}}{A_{\lambda_{2_{\mathrm{adj}}}}}$$

where

$$A_{\lambda_{\mathrm{adj}}} = \frac{A_{\lambda}}{C_{\mathrm{AuNP}}}$$

To test PG13T1 and PG13T2 selectivity for P4 relative to E2, we added the hormones separately to four AuNP solutions total, two for each aptamer. The LOD values for the P4 titrations were 0.55E-1nM and 0.65E-1nM for PG13T1 and PG13T2 respectively whereas the LOD values for the E2 titrations were 4.91E-1nM and 7.38E-1nM. This indicates that PG13T1 and PG13T2 were approximately ten times more sensitive to P4 than E2.

As the concentration of P4 increased, the ratio between the absolute absorption of two different wavelengths of light (523nm and 625nm) changed in a linear fashion. This suggests that the absorption spectra also changed in shape, resulting in color change. More and more aptamers dissociated from the gold nanoparticles and bound to the P4 molecules. This allowed increasing amounts of gold nanoparticles to aggregate.

PG13T2 exhibited a higher affinity for P4 than PG13T1 (Figure 6) because a larger slope (85.6E-4 for T2 compared to 60.8E-4 for T1) indicates that less P4 is needed to induce the same spectra shift and thus the same color change. We expected PG13T1 to be more specific to P4 than PG13T2 due to a higher Kd value [2]. Our results support the opposite, with PG13T2 being the more specific aptamer. However, with R^2 values of 0.818 and 0.83 for E2 and P4 respectively, PG13T2 appears to have more variance with regard to whether or not hormone concentration has a direct linear relationship with color change.

It was expected that the lines of best fit for the E2 titrations would have a slope with a smaller magnitude than the lines of best fit for the P4 titrations. This is because we want the relationship between E2 concentration and color change to be less pronounced than that for P4.

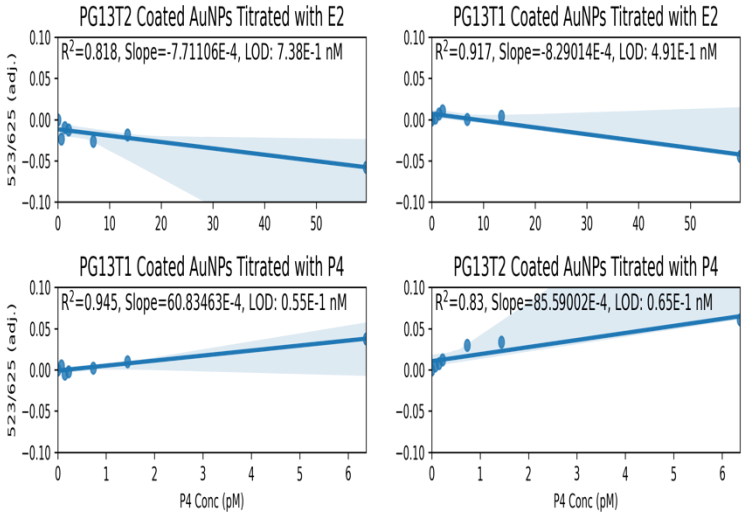

FIGURE 6. Titrations of P4/E2 in AuNP Solutions doped with PG13T1 or PG13T2 Aptamers. Graphs depict $A_{\lambda_1:\lambda_{2_{adj}}}$ at 523 and 625nm.

Conclusion

Our goal with this experiment was to identify new aptamers that exhibit high affinity and selectivity in the context of an AuNP assay for testosterone and progesterone. In doing so, we further our aim to develop a cheap, field ready, and rapid test for these hormones which can be used by trans people in "DIY-HRT" to aid them in making informed decisions.

The ideal assay enables detection of these specific hormones in application relevant solutions without additional equipment and here, a colorimetric aptamer-based method for detection is preferred for their high affinity, stability, and low production cost.

We identified two progesterone aptamer candidates, PG13T1 and PG13T2, and hypothesized that PG13T1 will exhibit higher selectivity for P4 than PG13T2 because of it's

slightly lower Kd value. After performing several titrations, we were able to refute our hypothesis because our results indicate that less P4 is needed for PG13T2 to induce the same spectra shift and thus the same color change as PG13T1 would need. Additionally, we discovered, by calculating and comparing their LOD values for P4 and E2, that the aptamers are approximately ten times more sensitive to P4 than E2.

We also identified four aptamer candidates for testosterone: JausetRubio2019-T6-46, JausetRubio2019-T6-54m, JausetRubio2019-T6-57, and JausetRubio2019-T6-60 through modifying a promising aptamer described in previous literature [3]. Due to COVID-19, we have not yet been able to test them.

In the near future, we plan to increase the number of repetitions of our experiment and test our synthesized testosterone aptamers to find out whether or not they exhibit high affinity and selectivity.

Acknowledgments

This research project was made possible by the Trans Is Becoming Institute of Casper, Wyoming.

References

[1] Rotondi, N. K., Bauer, G. R., Scanlon, K., Kaay, M., Travers, R., & Travers, A. (2013). Nonprescribed hormone use and self-performed surgeries: "do-it-yourself" transitions in transgender communities in Ontario, Canada. American journal of public health, 103(10), 1830–1836. https://doi.org/10.2105/AJPH.2013.301348

[2] Alhadrami, H. A., Chinnappan, R., Eissa, S., Rahamn, A. A., & Zourob, M. (2017). High affinity truncated DNA aptamers for the development of fluorescence based progesterone biosensors. Analytical biochemistry, 525, 78–84. https://doi.org/10.1016/j.ab.2017.02.014

[3] Jauset-Rubio, M., Botero, M. L., Skouridou, V., Aktas, G. B., Svobodova, M., Bashammakh, A. S., El-Shahawi, M. S., Alyoubi, A. O., & O'Sullivan, C. K. (2019). One-Pot SELEX: Identification of Specific Aptamers against Diverse Steroid Targets in One Selection. ACS omega, 4(23), 20188–20196. https://doi.org/10.1021/acsomega.9b02412

[4] Alsager, O. A., Kumar, S., Zhu, B., Travas-Sejdic, J., McNatty, K. P., & Hodgkiss, J. M. (2015). Ultrasensitive colorimetric detection of 17β-estradiol: the effect of shortening DNA aptamer sequences. Analytical chemistry, 87(8), 4201–4209. https://doi.org/10.1021/acs.analchem.5b00335

[5] Skouridou, V.; Jauset-Rubio, M.; Ballester, P.; Bashammakh, A. S.; El-Shahawi, M. S.;Alyoubi, A. O.; O'Sullivan, C. K. (2017). Selection and characterization of DNA aptamers against the steroid testosterone.184, 1631–1639. https://doi.org/10.1007/s00604-017-2136-0

[6] Qiao, L., Wang, H., He, J., Yang, S., & Chen, A. (2021). Truncated affinity-improved aptamers for 17β-estradiol determination by AuNPs-based colorimetric aptasensor. Food chemistry, 340, 128181. https://doi.org/10.1016/j.foodchem.2020.128181

[7] Liu, J., Bai, W., Niu, S., Zhu, C., Yang, S., & Chen, A. (2014). Highly sensitive colorimetric detection of 17β-estradiol using split DNA aptamers immobilized on unmodified gold nanoparticles. Scientific reports, 4, 7571. https://doi.org/10.1038/srep07571

[8] Prior, J. C. (2019). Progesterone Is Important for Transgender Women's Therapy—Applying Evidence for the Benefits of Progesterone in Ciswomen, The Journal of Clinical Endocrinology & Metabolism, Volume 104, Issue 4, April 2019, Pages 1181–1186, https://doi.org/10.1210/jc.2018-01777

[9] Zuker, M. Mfold web server for nucleic acid folding and hybridization prediction.31,3406–3415, Publisher: Oxford Academic.

[10] Zheng, Y., Wang, Y., & Yang, X. (2011). Aptamer-based colorimetric biosensing of dopamine using unmodified gold nanoparticles. Sensors and Actuators B: Chemical. https://www.sciencedirect.com/science/article/abs/pii/S0925400511002735.

[11] Pires, T. A., Narovec, C. M., Whelan, R. J. (2017) Effects of Cationic Proteins on Gold Nanoparticle/Aptamer Assays. ACS Omega 2 (11), 8222-8226. https://doi.org/10.1021/acsomega.7b01336

TABLE S1. Sequences for progesterone and testosterone aptamers. (*Tested, +Derivative Aptamer)

Aptamer	Target	Length	Sequence
Alhadrami2017-PG13	P4	61nt	GCATCACACACCGATACTCACCCGCCTGATTAAC ATTAGCCCACCGCCCACCCCCGCTGC
Alhadrami2017-PG13C4	P4	11nt	TGGGCGGTGGG
Alhadrami2017-PG13T1*	P4	31nt	GCATCACACACCGATACTCACCCGCCTGAT
Alhadrami2017-PG13T2*	P4	26nt	GATTAACATTAGCCCACCGCCCACC
JausetRubio2019-P5	T	100nt	TAGGGAAGAGAAGGACATATGATACCTCCGAAGT ATCATGCGGAGCATGTCCCGAATTTCATTCGTTC TCGTGACTTGACTAGTACATGACCACTTGAGG
JausetRubio2019-P6	T	88nt	TAGGGAAGAGAAGGACATATGATGTCTGAGGTAC TCACTTCTCACGTACGTTTCCCTCCTGAATTGAC TAGTACATGACCACTTGAGG
JausetRubio2019-T6-46^{+*}	T	46nt	GAAGAGAAGGACATATGATGTGCCGTGAATACAG GCCCTTCTCCGC
JausetRubio2019-T6-54m^{+*}	T	54nt	TAGGGAAGAGAAGGACATATGATGTGCCGTGAAT ACAGGCCCTTCTCTGCTCGT
JausetRubio2019-T6-57m^{+*}	T	57nt	AGAGAAGGACATATGATGTGCCGTGAATACAGGC CCTTCTCCGCTCCGCGTTCCGCT
JausetRubio2019-T6-60^{+*}	T	60nt	TAGGGAAGAGAAGGACATATGATGTGCCGTGAAT ACAGGCCCTTCTCCGCTCCGCGTTCC
Jauset-Rubio2019-T6*	T	86nt	TAGGGAAGAGAAGGACATATGATGTGCCGTGAAT ACAGGCCCTTCTCCGCTCCGCGTTCCGCTTTGAC TAGTACATGACCACTTGA
Skouridou2017-T5	T	86nt	TAGGGAAGAGAAGGACATATGATTGCGTGGGTAG GAAGGGGCGGTGTGATCTGAATCGTTCGATTGAC TAGTACATGACCACTTGA

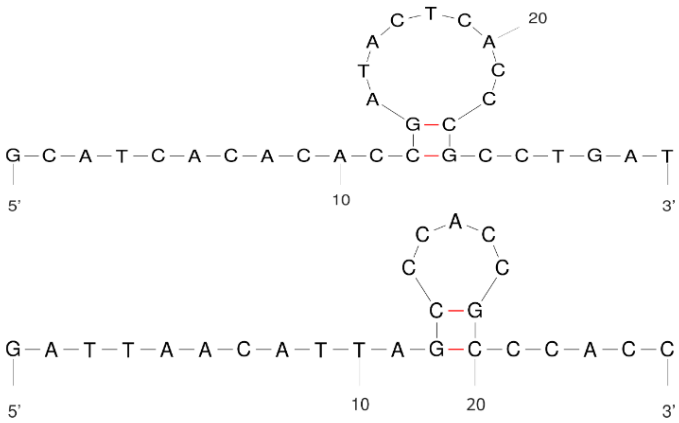

FIGURE S1. Simulated Secondary Structures of PG13T1 (top, ΔG=0.54) and PG13T2 (bottom, ΔG=-0.35).

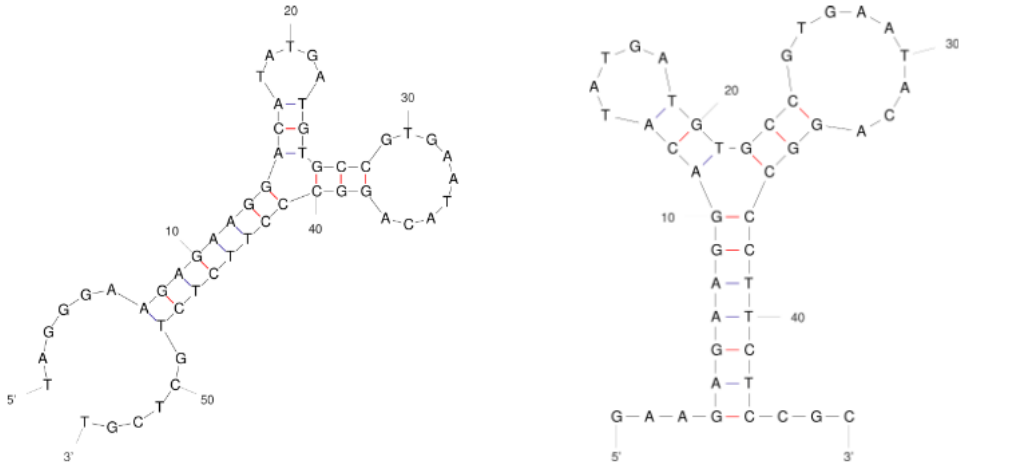

(a) JausetRubio2019-T6-54m (ΔG=-5.94) (b) JausetRubio2019-T6-46 (ΔG=-4.94)

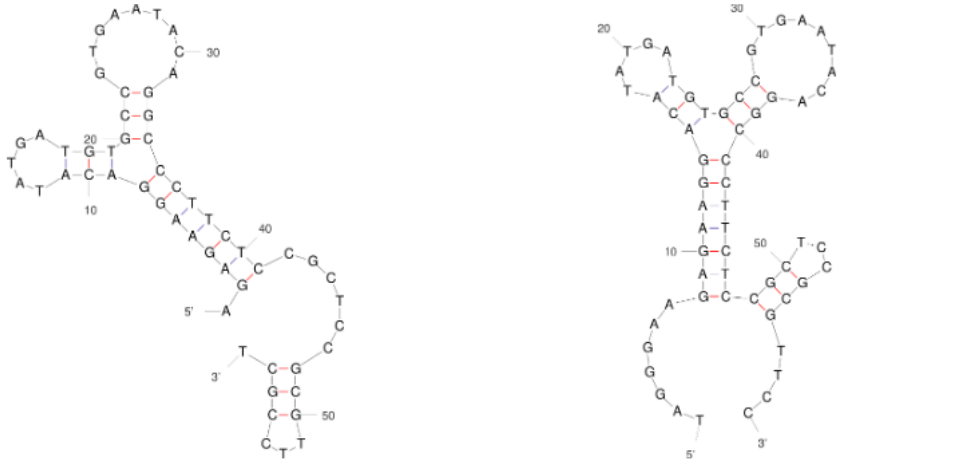

(c) JausetRubio2019-T6-57 (ΔG=-6.83) (d) JausetRubio2019-T6-60 (ΔG=-6.08)

FIGURE S2. Simulated Secondary Structures of Modified JausetRubio 2019-T6 Aptamers.

FIGURE S3. Simulated Secondary Structure of Skouridou2017-T5 (ΔG=-0.81).